PERGAMON

AE International – Central & South America

Atmospheric Environment 37 (2003) 183–193

ATMOSPHERIC ENVIRONMENT

www.elsevier.com/locate/atmosenv

A study of air flow patterns affecting pollutant concentrations in the Central Region of Mexico ☆

Aron D. Jazcilevich*, Agustín R. García, L. Gerardo Ruíz-Suárez

Centro de Ciencias de la Atmósfera, Universidad Nacional Autónoma de México, México, DF, 04510, Mexico

Received 15 April 2002; accepted 10 October 2002

Abstract

Using a prognostic air quality model that includes actual emissions, air pollution regimes over the central region of Mexico are simulated. It is shown that due to the complex orography, vertical circular patterns develop over the metropolitan area of Mexico City. In this way reactive and non-reactive pollutants can travel near the surface, be transported vertically and land in an area opposite to its initial route due to convective downward currents. This changes the surface pollutant concentrations on the landing area. Also, it is shown that air pollution is transported near the surface from the metropolitan area of Mexico City through Chalco in the South-east corner of the Mexico Valley, to the Valley of Cuautla affecting this area.

Keywords: Mexico City; Air pollution modeling; Air quality; Air flow in complex terrain

1. Introduction

Despite recent improvement in the air quality of Mexico City, the Valley of Mexico remains a highly polluted area. Levels of ozone (O_3) were above the WHO accepted standard for 300 days in 1999 (GDF, 1999). It is estimated that in the Metropolitan Area of Mexico City (MAMC) the population is about 18.5 million, with 3.8 million vehicles burning 44 million liters of fuel per day, plus the emissions of industrial and commercial activities that account for almost 30% of the GNP of Mexico (INEGI, 1999). Also the valley is surrounded by high mountains in the east, south and west, and to the north by lower discontinuous ranges, see Fig. 1. As will be shown here this orographic situation, besides tending to confine the air pollution, gives rise to intricate flows with consequences for the air quality of the MAMC and the contiguous Valley of Cuautla. The air pollution flows presented here provide new insights into the air pollution phenomenon of the central region of Mexico.

2. The air quality model

The air quality model used in this work is the Multi Scale Climate Chemistry Model (MCCM) that has been implemented for the central region of Mexico (Garcia et al., 2000) and used to study air pollution impact due to land use changes in the region Jazcilevich et al., (2002). A detailed description of the model can be found in Grell et al. (2000). For completeness we describe it here briefly.

The model includes modules for meteorology, photolysis, biogenic emissions, radiation, and deposition among others. The meteorological module of MCCM is based on the fifth-generation Penn State/NCAR Mesoscale Model called MM5 (see Grell et al., 1994). It is widely used by the meteorological community. MM5 is non hydrostatic with terrain following coordinates, has a multi-scale option, is capable of

☆ Partially supported by grant RI-500-5-1 CONACYT-RED.
*Corresponding author.
E-mail address: jazcilev@servidor.unam.mx (A.D. Jazcilevich).

1352-2310/02/$ - see front matter
PII: S1352-2310(02)00893-2

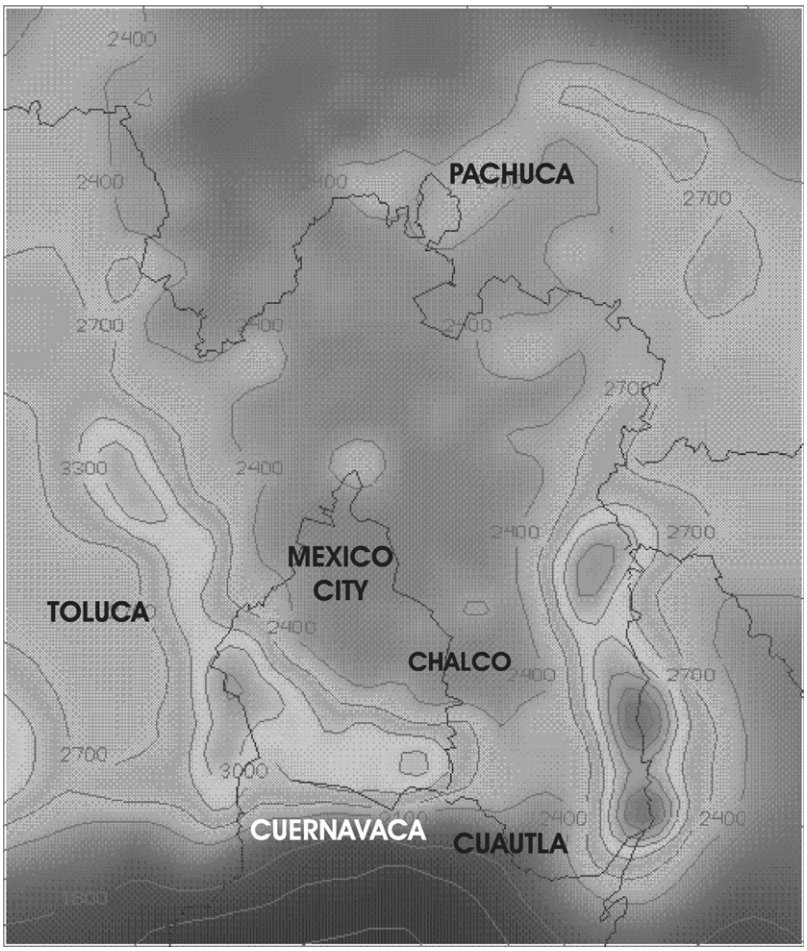

Fig. 1. The Valley of Mexico, its surrounding ranges and the Valleys of Cuautla and Cuernavaca in the South, Puebla in the East, and Toluca in the West.

four-dimensional data-assimilation, has an interface with actual weather forecast models (GCM and observations), contains explicit cloud schemes and multilevel soil/vegetation parameterization.

An advantage of MCCM is that the meteorological model is directly coupled with a chemistry-transport-model and a photolysis module. The biogenic emissions module is coupled with the radiation and RADM2 photochemistry modules (Stockwell et al., 1990). Also, a deposition module is coupled with higher order closure turbulence parameterization, a WALCEK aqueous phase chemistry extension to RACM can be used, and a third-order Smolarkiewicz scheme is used for pollutant advection. For a detailed description of this see (Grell et al., 2000).

The gas phase chemistry used in this study was RADM2, Stockwell et al. (1990). This mechanism considers for the inorganic part, 14 stable species, four reactive intermediaries and three abundant-stable species. The organic part considers 26 stable species and 16 peroxy radicals. The photo-chemistry is based on the aggregated molecular approach for reactivity (Middleton et al., 1990). The photolysis module uses a radiative transfer model. This module calculates photolysis frequencies for reaction gas phase chemistry that considers changes in the radiation with height and changes in air composition such as O_3, aerosols and water vapor. Local measurements of albedo found in Castro et al. (2001) are used.

The biogenic module calculates organic emissions of isoprene, monoterpenes and other organic and inorganic compounds such as nitrogen soil emissions. This kind of emission depends on temperature, radiation and type of vegetation. The dry deposition module calculates the elimination of trace compounds from the atmosphere depending on deposition velocity which is calculated using aerodynamic, sub-layer and surface resistance (Wesley, 1989).

3. Geographical setting and climate of the region

The MAMC lies on an inland basin called Valley of Mexico, elevated 2250 m above mean sea level in Central Mexico. Surrounding mountains reach to more than 2500 m above the basin floor. Low level regional winds from the NW during the cool season are usually not strong enough to provide ventilation becoming a contributing factor to the air pollution in the valley. This wind pattern is characteristic of a frontal passage. At other times weak regional winds give way to cool, thermally driven down-slope winds that during the night reinforce the Urban Heat Island induced centripetal circulation, thus contributing to the lateral confinement of air pollutants (Jauregui, 1988). Only in the South-eastern corner of the basin in the region of Chalco, relatively low height mountains allow for the possibility of pollutants drainage to the contiguous lower Valley of Cuautla to the SE, see Fig. 1.

The climate of the basin is wet-dry tropical in character (latitude 19.5N), tempered by altitude with a mean annual temperature of 16°C. During the dry season (November–April) clear skies and anti-cyclonic weather prevail with little rain falling during frontal passages. From May to October, the dry Westerlies give way to the moist trade wind current that brings convective rain showers. A marked rainfall gradient exists from the semiarid (400 mm/yr) center of the plains towards the south and west foothills, where orography and heat island effects enhance precipitation intensity to about 1000 mm/yr (Jauregui, 1986).

Since the simulations include days in the beginning of March a description of the climatology for this period of time follows: continental dry polar air masses from North-America sweep over the Basin of Mexico generating winds of moderate intensity (approximately 5 m s^{-1}). After a frontal passage, anti cyclonic weather prevails leading to the formation of surface-based radiation inversions (Jauregui, 1986), favoring high pollution episodes. A high daily temperature range is characteristic of this time of the year with typical maximum temperatures around 23°C, while minimum temperatures may reach near freezing during the night. The scant rains (about 5 mm) that fall are associated to frontal passages.

4. Experiment setup, input data and model performance

4.1. Setup of MCCM

The time period chosen for the computational experiments takes place from 2–5 March 1997, and corresponds to a high pressure anti-cyclonic system over the central region of Mexico providing favorable conditions for a typical high pollution scenario.

Three one-way nested domains are used as shown in Fig. 2 for the experiments. The horizontal resolution for the three domains are 27 km (D1), 9 km (D2), and 3 km (D3). This inner domain includes the Valley of Mexico with the metropolitan area of Mexico City, the mountain ranges surrounding it, and the cities of Cuernavaca and Toluca. There are 23 stretched vertical sigma levels with higher resolution near the ground with layer thickness of about 20 m. The uppermost level is at a height of about 100 mb. To initialize and to provide boundary values for MCCM, National Centers for Environmental Prediction (NCEP) historical archives were used with a time resolution of 6 h.

The first 24 h of modeling are used only for initialization. The boundary for Domain 3 was selected to include all important industrial and urban emissions in the central region of Mexico. Boundary concentration values for this domain are obtained from Domain 2 whose boundaries are set to background concentrations.

4.2. Emission inventory

The anthropogenic emissions inventory includes mobile, point and area sources. These data are obtained from emission inventories performed by the city government (GDF, 1995). The compounds considered are nitrogen oxides (NO_x), sulphur dioxide (SO_2), carbon monoxide (CO) and volatile organic compounds (VOC). The temporal resolution of the emissions model is 1 h and the spatial resolution is 2 km. The emissions inventory domain includes an area of $32,400\ km^2$.

Biogenic emissions mainly due to forests and farm-land are also considered in this work, and are obtained using the biogenic emission module mentioned earlier. Although the anthropogenic emissions are the main emission contribution, emissions from natural sources could represent, in some cases, an important source of VOC's (Ruiz-Suarez et al., 1999; Lamb et al., 1987).

4.3. Error analysis and performance of model output

Tables 1 and 2 show a statistical error analysis for modeled temperature and wind intensity, respectively, using data provided by stations of the local automatic monitoring network named RAMA. The statistics presented include the index of agreement d (see Willmott, 1981), which has an optimum value of 1.0 for perfect agreement between model and measurements.

It can be seen that d for temperatures is around 0.90 in all stations. For wind intensity d is above 0.50 in most stations and reaches above 0.65 for stations Tlalnepantla and Xalostoc. The overall average for the index of agreement d is 0.54. Similar satisfactory results were obtained for the other statistical parameters. It should be noted that all these statistical results are significantly

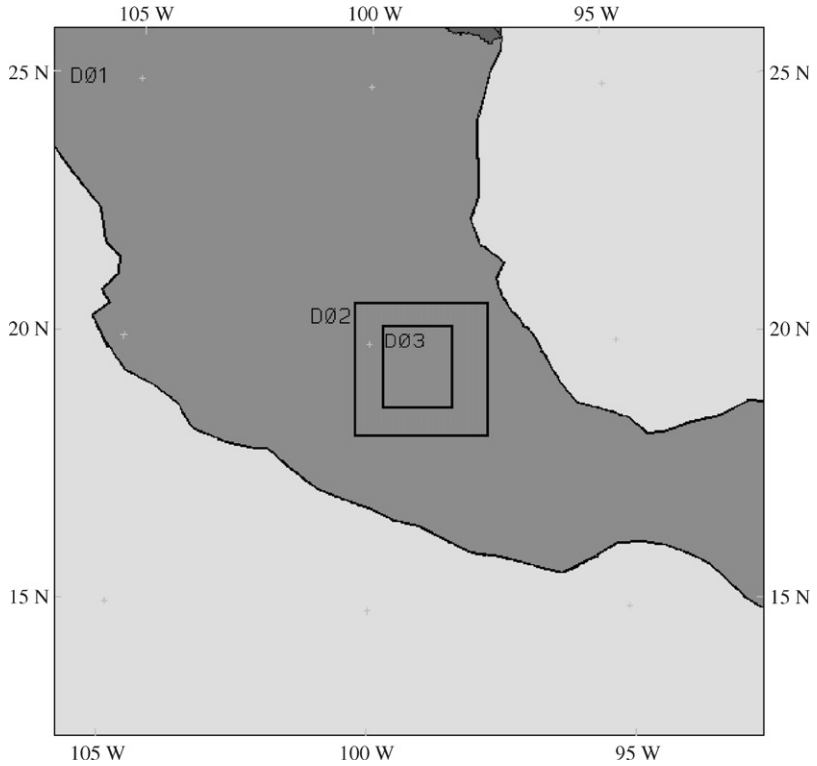

Fig. 2. Nested domains used to run the experiments. The largest domain has a resolution of 27 km, the next domain of 9 km, and the innermost 3 km.

Table 1
Statistical analysis for surface temperature; CC correlation coefficient, RMSE root mean square error, $RMSE_s$ root mean square error systematic, $RMSE_u$ root mean square error unsystematic, d index of agreement

Station	CC	d	RMSE	$RMSE_u$	$RMSE_s$	$RMSE_s/RMSE$	$RMSE_u/RMSE$
Tlalnepantla	0.86	0.87	3.68	2.99	2.14	0.81	0.58
Acatlan	0.86	0.88	3.74	3.06	2.16	0.82	0.58
Xalostoc	0.87	0.84	3.92	3.37	2.00	0.86	0.51
San Agustin	0.87	0.90	3.29	2.45	2.20	0.74	0.67
C. Estrella	0.88	0.90	3.25	2.54	2.04	0.78	0.63
Pedregal	0.91	0.90	2.84	2.34	1.62	0.82	0.57
Plateros	0.88	0.89	3.27	2.64	1.93	0.81	0.59
Merced	0.87	0.88	3.49	2.65	2.26	0.76	0.65
Hangares	0.86	0.90	3.03	2.25	2.03	0.74	0.67

better than other studies carried in the area, IMP-Los Alamos (1994) and comparable to the results in Jazcilevich et al. (2002). Table 3 shows a statistical analysis for O_3 for same RAMA stations as above. In most stations values for d above 0.70 were achieved with an overall average value of 0.78. Similar good results were obtained for the other statistical parameters.

Fig. 3 shows time series for modeled and measured surface temperatures for selected RAMA stations. Fig. 4 shows time series comparing measured and modeled O_3 concentrations for the same selected RAMA stations. Fig. 5 shows a comparison of the vertical profile of measured and modeled temperatures and wind intensity at the International Airport of Mexico City at 18:00 LST, 2 March 1997. These figures, together with the statistical analysis show that the model is satisfactorily reproducing the meteorological and pollution phenomena in the valley.

Table 2
Statistical analysis for surface wind intensity; CC correlation coefficient, RMSE root mean square error, $RMSE_s$ root mean square error systematic, $RMSE_u$ root mean square error unsystematic, d index of agreement

Station	CC	d	RMSE	$RMSE_u$	$RMSE_s$	$RMSE_s/RMSE$	$RMSE_u/RMSE$
Tlalnepantla	0.43	0.65	1.21	0.73	0.96	0.60	0.80
Acatlan	0.24	0.53	1.23	0.78	0.94	0.64	0.77
Xalostoc	0.44	0.66	1.21	0.77	0.94	0.63	0.77
San Agustin	0.30	0.57	1.18	0.75	0.91	0.64	0.77
C. Estrella	0.39	0.46	1.20	0.63	1.02	0.53	0.85
Pedregal	0.46	0.58	0.84	0.46	0.71	0.54	0.84
Plateros	0.25	0.50	1.09	0.72	0.82	0.66	0.75
Merced	0.61	0.37	1.09	0.47	0.98	0.43	0.90
Hangares	0.25	0.54	1.47	1.05	1.04	0.71	0.70

Table 3
Statistical analysis for surface O_3; CC correlation coefficient, RMSE root mean square error, $RMSE_s$ root mean square error systematic, $RMSE_u$ root mean square error unsystematic, d index of agreement

Station	CC	d	RMSE	$RMSE_u$	$RMSE_s$	$RMSE_s/RMSE$	$RMSE_u/RMSE$
Tacuba	0.77	0.83	0.04	0.03	0.03	0.67	0.76
Acatlan	0.74	0.82	0.04	0.03	0.03	0.68	0.71
San Agustin	0.69	0.72	0.04	0.02	0.03	0.59	0.80
Azcapotzalco	0.73	0.69	0.04	0.03	0.03	0.73	0.70
Xalostoc	0.60	0.67	0.05	0.03	0.04	0.58	0.82
Merced	0.71	0.83	0.04	0.03	0.02	0.79	0.59
C. Estrella	0.70	0.80	0.04	0.03	0.03	0.73	0.70
Lagunilla	0.68	0.79	0.05	0.03	0.03	0.70	0.70
Tlalnepantla	0.79	0.86	0.03	0.02	0.02	0.77	0.63
Pedregal	0.82	0.84	0.04	0.02	0.03	0.56	0.82

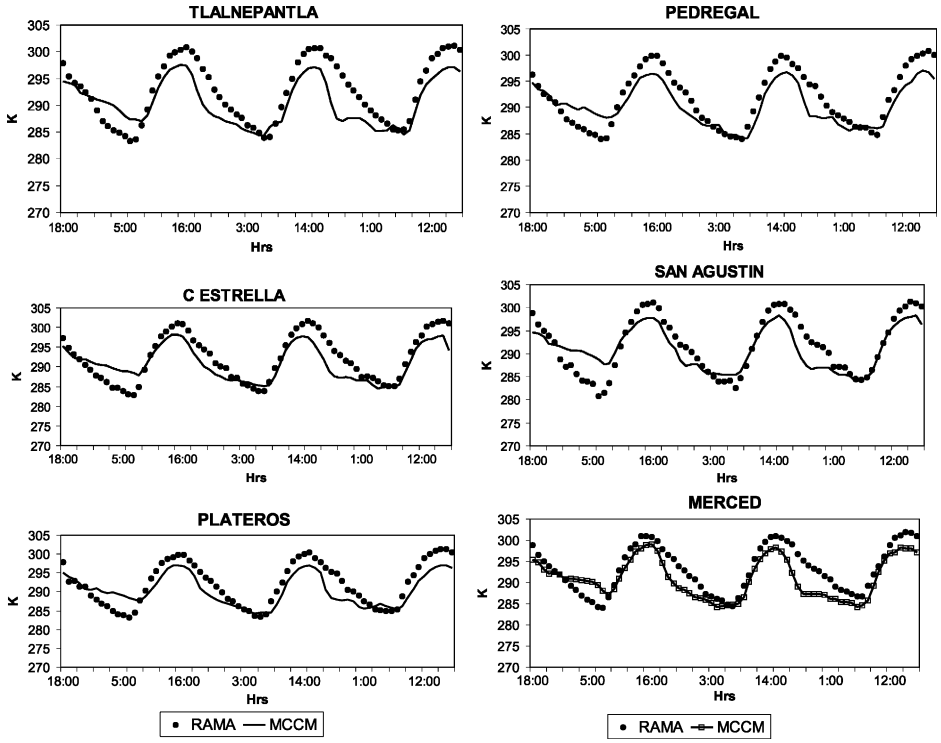

Fig. 3. Temperature profiles using MCCM and measurements at selected RAMA stations.

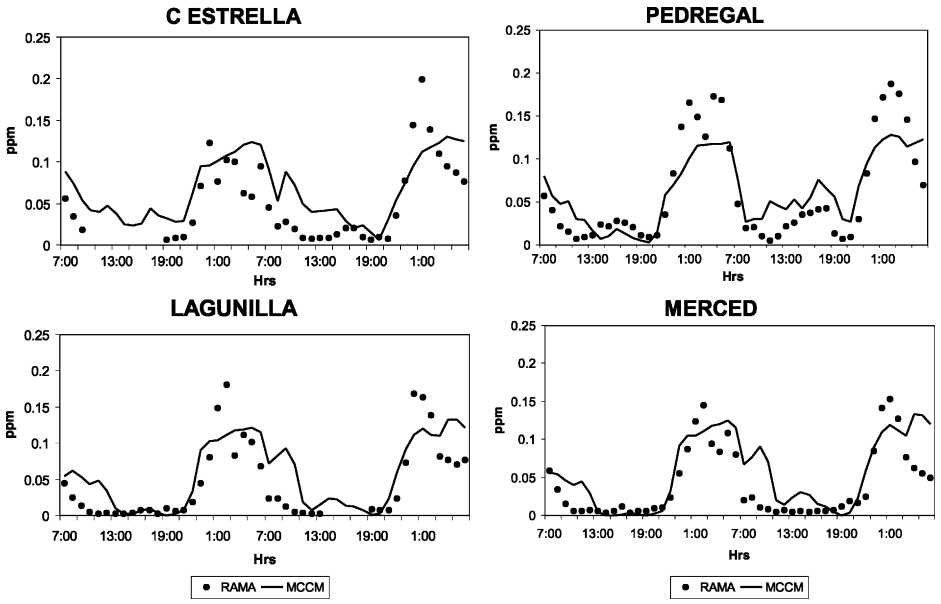

Fig. 4. Ozone concentrations for 60 h using MCCM and measurements at some selected RAMA stations in ppm.

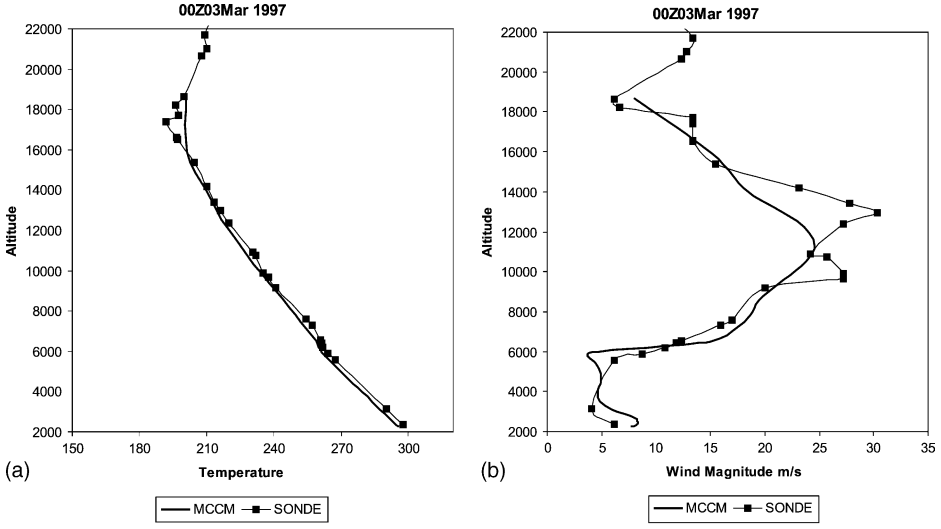

Fig. 5. Vertical profiles comparing measured and modeled temperatures in (a), and wind velocity in (b) at the International Mexico City Airport at 18 LST 2 March 1997.

5. Results

5.1. Vertical circular wind flows over the MAMC

Fig. 6 shows a North-east to South-west vertical slice where we can see the vertical wind flow over the MAMC at 21:00 LST, 2 March 1997. A vertical circular wind pattern is revealed. This figure also shows how CO emitted at the surface has been transported first from the center of the MCCM, the area with highest emissions, to the South-West corner of the MAMC. CO is then advected up vertically due to the presence of the Ajusco ridge. Once on a higher atmospheric layer at a height of about 900 m above the basin floor, it is transported back to the North-east passing over the surface path it covered initially, and finally descends convectively on

the North-eastern corner of the MAMC. CO concentrations in the landing area are significant at about 8 ppm. Fig. 7(a) shows a similar pattern followed by NO_2. In Fig. 7(b), depleted concentrations of O_3 due to the presence of NO on its path, follow the same circular pattern. These patterns reveal that it is due to convective fumigation that change in pollutant concentrations on the surface takes place.

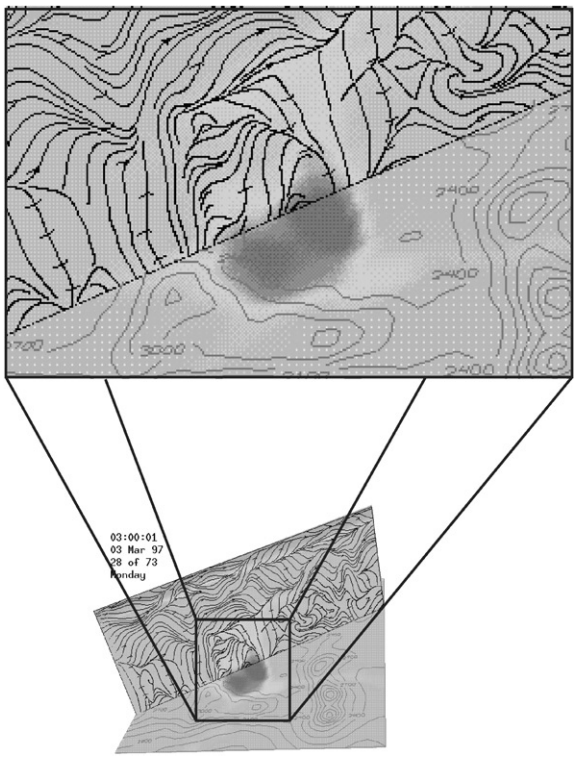

Fig. 6. North-east to South-west vertical slice and an enlargement of the area of interest over the MAMC at 21:00 LST, 2 March 1997. A vertical circular wind pattern can be seen transporting CO concentrations. On the landing area the darker color show that concentrations of CO reach 8 ppm.

To illustrate that we have vertical advection near the mountains followed by a convective downdraft, Fig. 8 shows that the potential temperature isotherm for 312 K is on the same path followed by the pollutants discussed above. Therefore, we can conclude that cold air is transported up vertically due to mechanical advection when air parcels are pushed against the mountains and once in the upper atmosphere these parcels tend to descend since they are colder than the surrounding air. This phenomenon occurs at night when the atmosphere is stable allowing for a descending current.

5.2. Pollution transport between the valleys of Mexico and Cuautla

A second pattern is shown in Fig. 9 where the surface wind flow and surface concentrations of CO are depicted over the central region of Mexico at 2:00 LST on the 4 March 1997. The same figure shows the location of a virtual surface station P1 on the Chalco area. This figure shows how CO is transported through Chalco to the Valley of Cuautla. Fig. 10 shows a vertical profile of CO concentrations and potential temperature at the P1 location. A temperature inversion is present at this time, promoting surface pollutant concentrations.

Fig. 11 shows the time series for CO, O_3, NO_x and SO_2 concentrations at P1. Peak concentrations of CO, SO_2 and NO are at 2:00 LST on the 4 March 1997, showing that maximum transport of pollutants in this

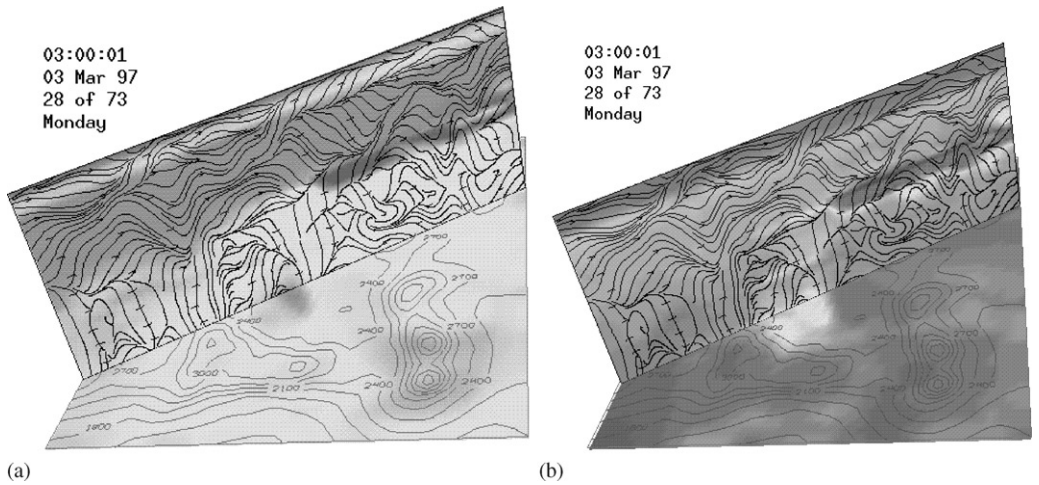

Fig. 7. North-east to South-west vertical slice over the MAMC at 21:00 LST, 2 March 1997. In (a) NO_2 is transported in a similar way as was described for CO. In (b), depleted concentrations of O_3 are transported in a similar fashion.

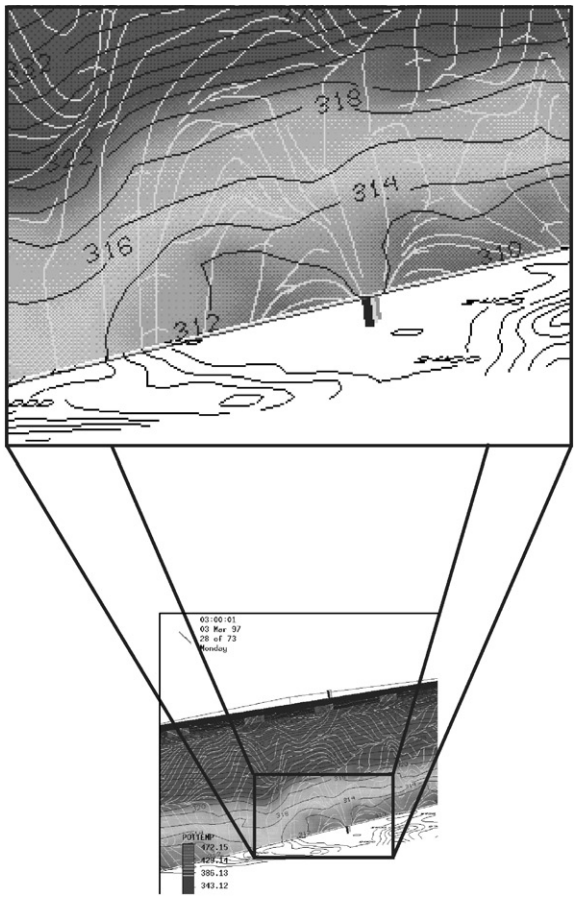

Fig. 8. North-east to South-west vertical slice and an enlargement of the area of interest over the MAMC at 21:00 LST, 2 March 1997, showing potential temperatures. The isotherm for 312 K is on the vertical circular path followed by the pollutants.

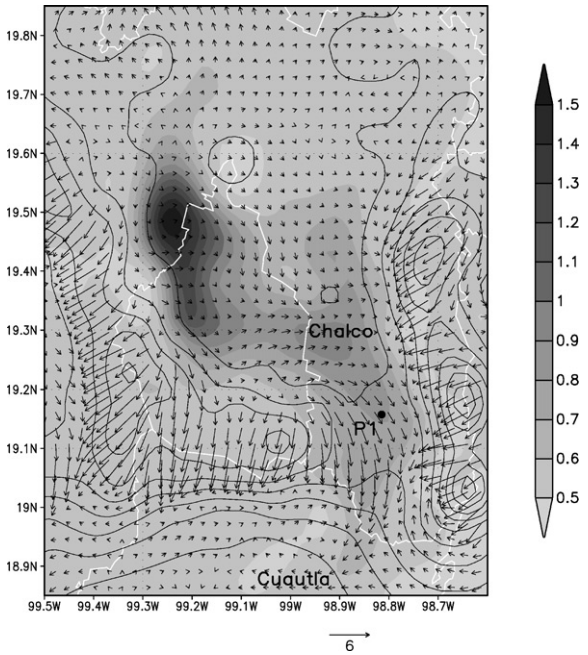

Fig. 9. Surface wind flow and CO surface concentrations over the central region of Mexico at 2:00 LST, 4 March 1997. P1 is a surface virtual station on the Chalco area. Note how CO concentrations drain through Chalco to the Valley of Cuautla.

site is at this time. Concentrations of O_3 are depleted because of the presence of NO there at this time.

Fig. 12 shows a North–South vertical slice passing over P1 also at 2:00 LST, showing a vertical profile of CO concentrations and potential temperature. Since the mixing layer height is low at this time, almost all transport takes place near the surface. Clearly, pollutants are transported to the Valley of Cuautla affecting this region.

6. Conclusion

The MAMC is situated in a complex orographic area causing intricate wind flows and pollutant transport. The first pollution flow pattern reveals how reactive and non-reactive pollutants can travel near the surface, be transported vertically and land in an area opposite to its initial route due to convective downward currents. Similar flow patterns in the region for other dates are described in Bossert (1997), and Fast and Zhong (1999), although inert tracing particles instead of actual emissions were used and no landing of pollutants due to downward convection currents was noticed. Only the possibility of fumigation by downward vertical diffusion of pollutants was mentioned there. In our simulations we not only observed this phenomenon, but also the existence fumigation by downward convective currents.

As the results of our modeling show, the amount of pollution brought down by convective currents is much more significant than the amount that could be carried down by vertical diffusion. The convective landing of reactive and non-reactive pollutants can explain sudden significant changes in concentration levels in some specific areas and represents an additional factor to be taken into account in order to understand the behavior of the air pollution phenomenon in the MAMC.

The second flow pattern shows how pollution in the Valley of Mexico can be transported through Chalco, whose height above MSL is 2200 m, to the Valley of Cuautla that lies approximately 900 m lower. The pollutant transport is near the surface, directly affecting this area. It happens mainly in the early morning at 2:00

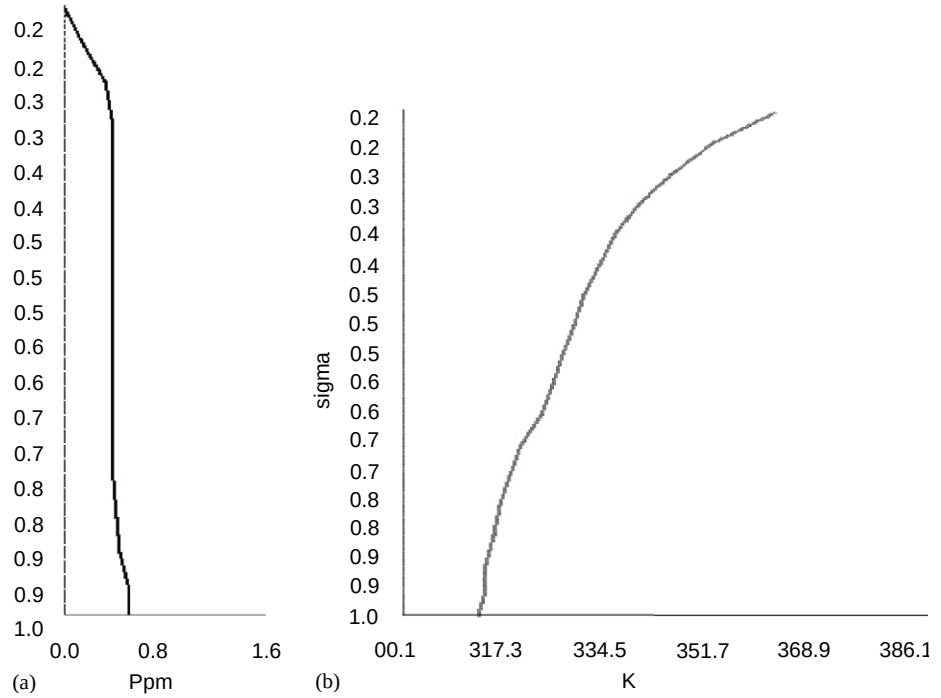

Fig. 10. Vertical profile in Sigma coordinates in (a) of CO concentrations in ppm and in (b) of potential temperatures in K, over the virtual surface station P1.

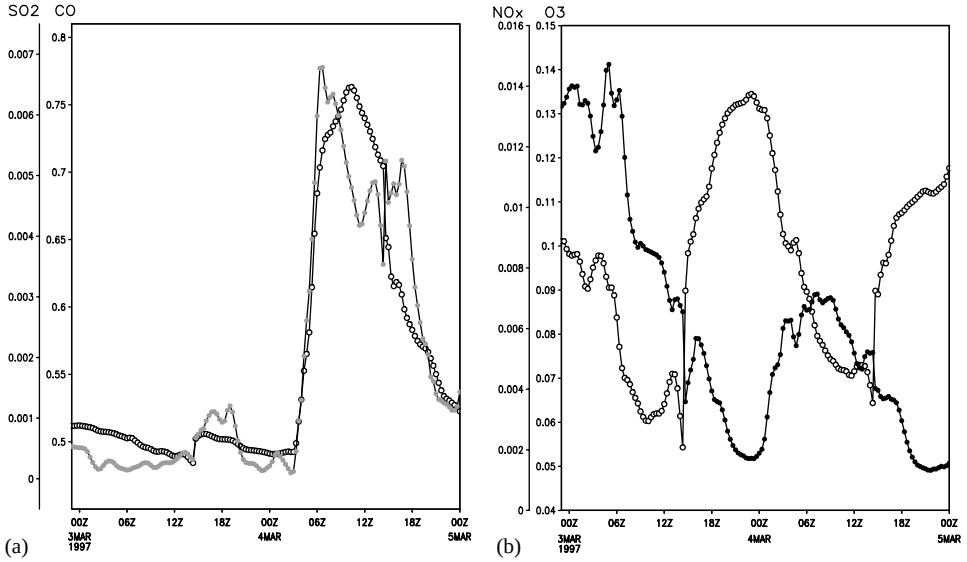

Fig. 11. Time series in (a) for CO (●), SO_2 (◦), and in (b) for O_3 (●) and NO_x (○) concentrations in ppm for last 48 h at virtual surface site P1 near Chalco. A peak in all pollutants except O_3 appears at 2:00 LST (GMT—6 h), 4 March 1997.

LST of 4 March 1997, leaving pollutants and precursors in the local area of Cuautla ready to photo-react in the morning. No measurements of this phenomenon have been carried out either in Chalco or Cuautla, but this simulation points out that this may be an important task for future measurement campaigns. This pattern shows

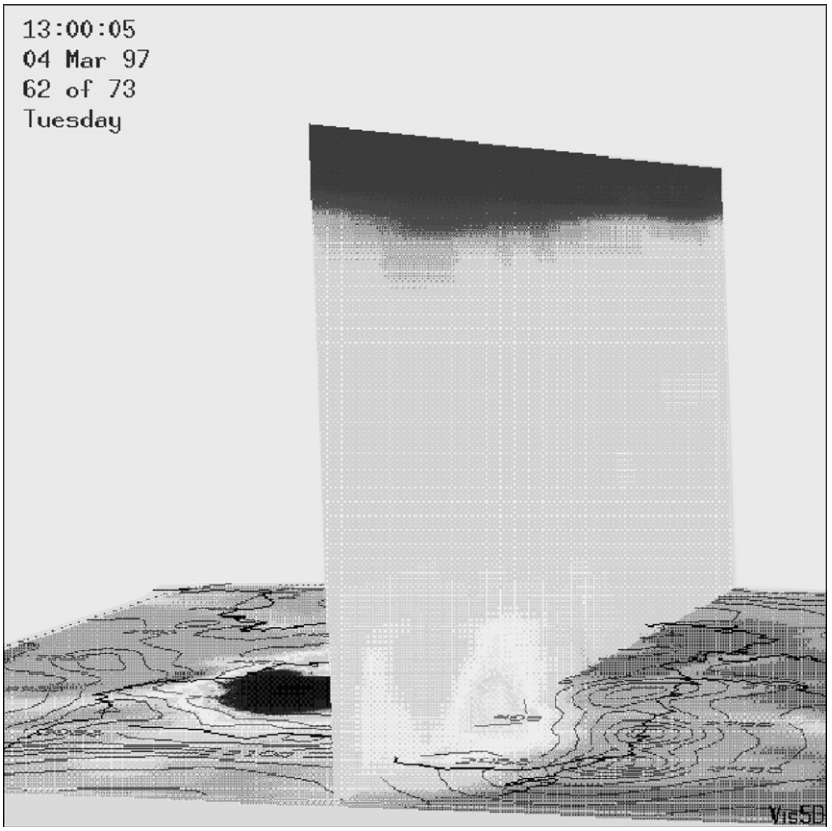

Fig. 12. North–South vertical slice passing over P1 also at 2:00 LST showing CO concentrations.

that although the pollution in the MAMC tends to be confined in the Valley of Mexico due to its orography, it can have an important effect in the surrounding valleys.

The simulations show how different areas of the central region of Mexico interact and how the abatement of pollution emissions in one region can reduce concentrations in another area and vice versa; if emissions are not controlled in one area, another region can be affected in intricate ways.

Acknowledgements

Thanks go to Renate Forkel of the Institut für Meteorologie und Klimatforschung, Btreich Atmospharische Umweltforschung (IMK-IFU), for her assistance running MCCM.

References

Bossert, J.E., 1997. An investigation of flow regimes affecting the Mexico City region. Journal of Applied Meteorology 36 (2), 119–140.

Castro, T., Mar, B., Longoria, R., Morales, L., Ruiz-Suarez, L.G., 2001. Surface albedo measurements in Mexico City metropolitan area. Atmosfera 14 (2), 69–74.

Fast, J.D., Zhong, S., 1999. Meteorological factors associated with inhomogeneous ozone concentrations within Mexico City basin. Journal of Geographical Research 103 (D15), 18927–18946.

Garcia, R.A., Schoenemyer, T., Jazcilevich, A., Ruiz-Suarez, D.G., Fuentes-Gea, V., 2000. In: Longhurst, J.W.S., Brebbia, C.A., Power, H. (Eds.), Implementation of the Multiscale Climate Chemistry Model (MCCM) for Central Mexico, Air Pollution VII, WIT Press, Southampton, pp. 71–78, ISBN 1-85312-822-8.

GDF (Gobierno del Distrito Federal), 1995. Inventario de fuentes de area precursores de ozono y monoxido de carbono para la zona metropolitana de la ciudad de México 1995, DDF-Subdireccion de inventario de emisiones.

GDF, Gobierno del Distrito Federal, 1999. Compendio Estadistico de la Calidad del Aire, 1986–1999. Secretaria del Medio Ambiente, p. 25.

Grell, G.A., Dudhia, J., Stauffer, D.R., 1994. A description of the fifth-generation Penn State/NCAR Mesoscale Model (MM5). NCAR Thecnical Note TN-398 + SRT.

Grell, G.A., Emeis, S., Stockwell, W.R., Schoenemeyer, T., Forkel, R., Michalakes, J., Knoche, R., Seidl, W., 2000. Application of a multiscale, coupled MM5/Chemistry

model to the complex terrain of the VOLTAP valley campaign. Atmospheric Environment 34, 1435–1453.

IMP, Instituto Mexicano del Petroleo, Los Alamos National Laboratory, 1994. Mexico City Air Quality Research Initiative, LA-12699, Vol III.

INEGI, 1999. Sistema de Cuentas Nacionales de Mexico:1993–1997, PIB por entidad federativa.

Jauregui, E., 1986. The Urban Climate of Mexico City. Technical Conference in Urban Climatology, WMO-652, pp. 26–45.

Jauregui, E., 1988. Local wind and air pollution interaction in the Mexico Basin. Atmosfera 1, 131–140.

Jazcilevich, D.A., Garcia, A., Gerardo Ruiz-Suarez, L., 2002. A modeling study of air pollution through land-use change in the Valley of Mexico. Atmospheric Environment 36, 2297–2307.

Lamb, B., Geuther, A., Gay, D., Westberg, H., 1987. A national inventory of biogenic hydrocarbon emissions. Atmospheric Environment 21, 1695–1705.

Middleton, P., Stockwell, W.R., Carter, W.P.L., 1990. Aggregation and analysis of volatile organic compound emissions for regional modeling. Atmospheric Environment 24A, 1107–1133.

Ruiz-Suarez, L.G., Longoria, R., Hernandez, F., Segura, E.H., Trujillo, A., Conde, C., 1999. Emisiones biogenicas de hidrocarburos no-metano y de oxido nitrico en la cuenca del valle de Mexico. Atmosfera 12, 89–100.

Stockwell, W.R., Middleton, R.P., Chang, J.S., Tang, X., 1990. The second generation regional acid deposition model chemical mechanism for regional air quality modeling. Journal of Geophysical Research 95, 16343–16367.

Wesley, M.L., 1989. Parametrization of surface resistance to gaseous dry deposition in regional numerical models. Atmospheric Environment 16, 1293–1304.

Willmott, C.J., 1981. On the validation of models. Physical Geography 2, 184–194.